

RESEARCH ARTICLE

## Sertraline Adsorption on the Surface of BN Nanocluster: A Comprehensive Theoretical Study

Mohamed Abu Shuheil<sup>1</sup>, Sheida Ahmadi<sup>2</sup>, Fatemeh S. Hosseininasab<sup>3</sup>, Huseyn A. Imanov<sup>4</sup>, Esmail Vessally<sup>2</sup>, Ali Z. Zalov<sup>5</sup>, Afet T. Huseynova<sup>6</sup>, Mohammad Reza Jalali Sarvestani<sup>7\*</sup>

<sup>1</sup> Faculty of Allied Medical Sciences, Hourani Center for Applied Scientific Research, Al-Ahliyya Amman University, Amman, Jordan

<sup>2</sup> Department of Chemistry, Payame Noor University, Tehran, Iran

<sup>3</sup> Department of Agriculture, Minab Higher Education Centre, University of Hormozgan, Bandar Abbas, Iran

<sup>4</sup> Department of Chemistry, Faculty of Natural Sciences and Agriculture, Nakhchivan State University, Nakhchivan, Azerbaijan

<sup>5</sup> Azerbaijan State Pedagogical University, AZ 1000, U. Hajibekova St.68, Baku, Azerbaijan

<sup>6</sup> Department of Organic Chemistry, Baku State University, Azerbaijan

<sup>7</sup> Young Researchers and Elite Club, YI.C., Islamic Azad University, Tehran, Iran

### ARTICLE INFO

#### Article History:

Received 05 Sep 2025

Accepted 21 Nov 2025

Published 01 Dec 2025

#### Keywords:

Sertraline  
Adsorption  
Removal  
 $B_{12}N_{12}$   
DFT  
Detection

### ABSTRACT

This research explored the capability of the boron nitride nanocluster ( $B_{12}N_{12}$ ) to act as an efficient adsorbent and sensor for detecting and removing the antidepressant drug sertraline (ST) using density functional theory (DFT) calculations. The study examined the interaction between ST and  $B_{12}N_{12}$  in different orientations, finding that the nanocluster has a stronger attraction to the chlorine atoms in ST. The negative values of adsorption energy, Gibbs free energy changes, and enthalpy changes indicate that the interaction is experimentally achievable, spontaneous, and exothermic. Additional analysis evaluated temperature effects and the role of water as a solvent, revealing that adsorption is more effective at lower temperatures and remains feasible in aqueous environments. Furthermore, the bandgap of  $B_{12}N_{12}$ , initially 6.664 eV, was significantly reduced to 4.963 eV after ST adsorption, representing a 25.530% decrease and a marked improvement in electrical conductivity. These results highlight  $B_{12}N_{12}$  as a promising material for applications in sertraline detection and removal, serving as both an adsorbent and a sensor.

### How to cite this article

Abu Shuheil M., Ahmadi S., Hosseininasab FS, Imanov HA, Vessally E., Zalov AZ., Huseynova AT, Jalali Sarvestani MJ. Sertraline Adsorption on the Surface of BN Nanocluster: A Comprehensive Theoretical Study. *Nanomed Res J*, 2025; 10(4): 407-415. DOI: 10.22034/nmrj.2025.04.008

## INTRODUCTION

The creation of innovative materials for use in environmental and pharmaceutical fields has become a central area of interest within the scientific community [1]. Among these, nanostructures have garnered significant attention due to their distinct physical and chemical characteristics, which make them highly suitable for diverse applications such as drug delivery, catalysis, adsorption, and sensing [2]. One particularly notable group of nanomaterials is boron nitride nanoclusters (BNNCs). These

materials stand out due to their remarkable thermal stability, chemical resistance, large surface area, and adjustable electronic properties [3]. In this research, we investigate the potential of the boron nitride nanocluster  $B_{12}N_{12}$  (Fig. 1) as a material for both adsorbing and detecting sertraline, a widely utilized pharmaceutical compound [4]. Sertraline (ST, Fig. 1), a selective serotonin reuptake inhibitor (SSRI), is a widely prescribed pharmaceutical agent primarily used to treat major depressive disorder, generalized anxiety disorder, panic disorder, social anxiety disorder, and other

\* Corresponding Author Email: [Rezajalali93@yahoo.com](mailto:Rezajalali93@yahoo.com)

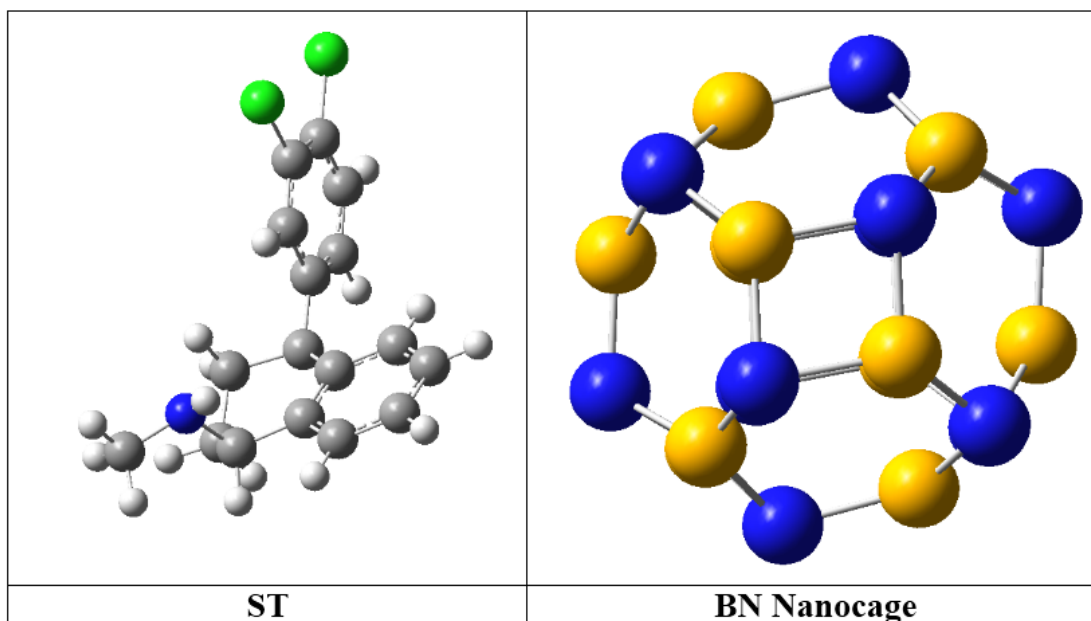


Fig. 1. Optimized structures of ST and  $B_{12}N_{12}$  (gray: carbon, white: hydrogen, green: chlorine, blue: nitrogen, yellow: boron)

mental health conditions such as obsessive-compulsive disorder (OCD) and post-traumatic stress disorder (PTSD) [5]. Its mechanism of action involves inhibiting the reuptake of serotonin in the brain, thereby increasing the availability of this neurotransmitter and promoting mood stabilization and emotional well-being. Due to its efficacy and relatively favorable side-effect profile compared to older antidepressants such as tricyclic antidepressants (TCAs) and monoamine oxidase inhibitors (MAOIs), sertraline has become a cornerstone in the pharmacological management of mood and anxiety disorders [6]. However, the widespread and long-term use of sertraline has raised significant environmental concerns. Research has shown that trace amounts of sertraline, along with its metabolites, are frequently detected in various environmental compartments, including wastewater, surface water, sediments, and even drinking water sources [7]. This contamination stems from the incomplete removal of pharmaceuticals during conventional wastewater treatment processes, which are not specifically designed to target these emerging pollutants. As a result, sertraline residues can persist in aquatic ecosystems, potentially affecting non-target organisms such as fish, invertebrates, and algae by interfering with their serotonin signaling pathways [5]. The ecological consequences of chronic

exposure to low concentrations of SSRIs like sertraline are still being investigated, but studies suggest that such exposure may alter behavior, reproduction, and survival rates in aquatic species. Furthermore, the presence of pharmaceuticals in drinking water raises public health concerns, as the long-term effects of consuming trace levels of these compounds remain unclear [6]. Addressing this issue will require advancements in wastewater treatment technologies, such as the implementation of advanced oxidation processes, membrane filtration systems, or other innovative methods capable of effectively removing pharmaceuticals from water sources. Additionally, increased public awareness about proper disposal of unused medications and stricter regulations on pharmaceutical waste management could help mitigate the environmental impact of sertraline and other similar compounds [7]. As research continues to explore the environmental and ecological implications of pharmaceutical contamination, it is imperative for scientists, policymakers, healthcare providers, and the public to collaborate in developing sustainable solutions that balance the therapeutic benefits of medications like sertraline with their potential impact on ecosystems and human health. The occurrence of sertraline in aquatic systems poses potential threats to ecosystems and human health, emphasizing the

urgent need to develop effective techniques for its detection and elimination [8].

Conventional techniques for eliminating pharmaceuticals from water include advanced oxidation processes [9], membrane-based filtration systems [10], and adsorption using activated carbon or other porous substances [8]. Although these methods can be effective to a degree, they often face challenges such as high energy requirements, the risk of secondary contamination, or inadequate selectivity [11]. In light of these limitations, nanomaterials such as BNNCs present a promising alternative due to their exceptional adsorption capacity, high selectivity, and ability to interact with specific molecular targets via chemical or physical mechanisms. BNNCs consist of boron and nitrogen atoms alternately arranged in a hexagonal lattice structure [12]. The distinctive structure of BNNCs endows them with exceptional traits such as a large bandgap, impressive mechanical durability, and outstanding chemical resilience [13]. Among these, the  $B_{12}N_{12}$  nanocluster has garnered significant attention due to its symmetric architecture and advantageous electronic properties [14]. Its expansive surface area and abundance of active sites make it highly suitable for applications in adsorption and sensing [15]. Furthermore,  $B_{12}N_{12}$  demonstrates robust interactions with various organic compounds through mechanisms like hydrogen bonding,  $\pi$ - $\pi$  stacking, and van der Waals forces, enhancing its effectiveness as both an adsorbent and a sensor [16]. Density functional theory (DFT) has emerged as a critical approach for exploring the atomic-level interaction mechanisms between nanomaterials and target molecules [17-20]. DFT sheds light on essential factors such as electronic configurations, binding energies, charge transfer, and other parameters influencing adsorption and sensing behaviors [21-23]. Through DFT modeling, researchers can anticipate how nanomaterials will perform in specific applications and refine their designs to achieve greater functionality and efficiency [24-28]. This study delves into a detailed DFT analysis of the interaction between the  $B_{12}N_{12}$  nanocluster and ST. By showcasing the dual role of  $B_{12}N_{12}$  as both an adsorbent and a sensor, this research adds valuable insights to the expanding field of nanomaterial-based approaches aimed at tackling environmental issues linked to pharmaceutical pollution.

### Computational Methods

The structural design and analysis of ST,  $B_{12}N_{12}$ , and their combinations were thoroughly performed using GaussView 6 [29] along with Nanotube Modeler 1.3.0.3. The process began with the geometric optimization of each structure to ensure their stability and to enable precise analysis. Once optimized, various computational studies were carried out, including infrared (IR) spectroscopy and frontier molecular orbital (FMO) analysis. Computational simulations were executed using the Gaussian 16 software suite [30], which is recognized for its advanced quantum chemical capabilities. Furthermore, density of states (DOS) spectra were analyzed with the help of GaussSum 03. The primary computational method employed was Density Functional Theory (DFT) [31], a quantum mechanical approach that solves the Kohn-Sham equations to calculate electronic structures. DFT is particularly suitable for studying adsorption processes due to its efficiency and accuracy when applied to systems with medium to large molecular sizes. For this research, the 6-31G\* basis set [32] was used for all calculations.

This split-valence basis set integrates polarization functions on heavier atoms, which are essential for accurately capturing electronic distributions and interaction energies in systems containing heteroatoms like boron and nitrogen. The 6-31G\* basis set strikes a balance between computational efficiency and accuracy, making it ideal for studying adsorption behaviors on nanoclusters. For this research, the exchange-correlation functional used was the B3LYP [33] hybrid functional, combining Becke's three-parameter exchange functional with the Lee-Yang-Parr correlation functional. The B3LYP functional is highly regarded in computational chemistry for its consistency in predicting molecular properties such as adsorption energies and thermodynamic data. To incorporate solvation effects, calculations were conducted in both gas and aqueous phases using the Conductor-like Polarizable Continuum Model (CPCM) [34-37]. Thermodynamic parameters were evaluated at three temperatures: 298 K, 308 K, and 318 K.

The process examined by [38-44] is as follows:  
 $ST + B_{12}N_{12} \rightarrow ST-B_{12}N_{12}$  (1)

## RESULTS AND DISCUSSION

### Structural Analysis

The interaction between ST and  $B_{12}N_{12}$  was

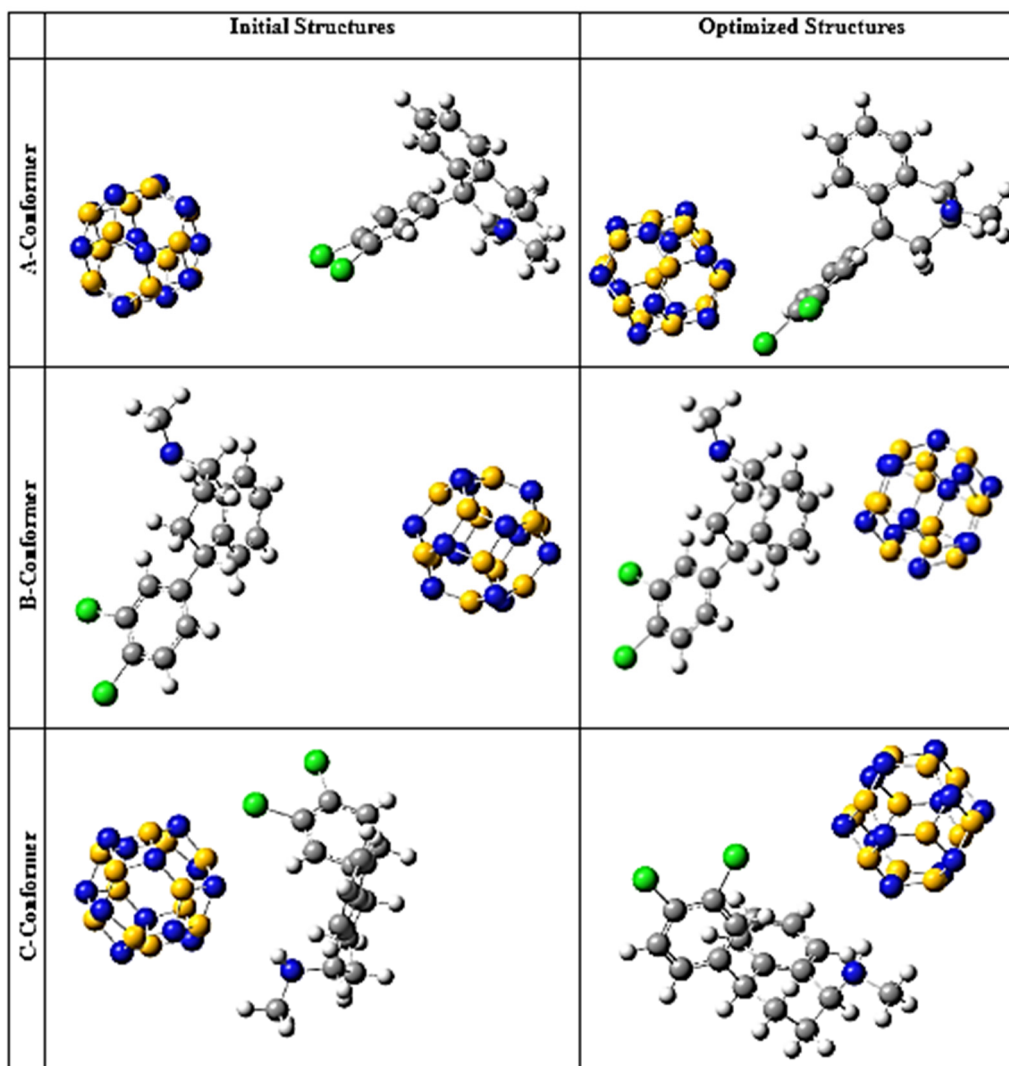


Fig. 2. Initial and optimized structures of ST- $B_{12}N_{12}$  Complexes (gray: carbon, white: hydrogen, green: chlorine, blue: nitrogen, yellow: boron)

thoroughly investigated by examining various orientations and conformers to pinpoint the most stable configurations. Out of all the conformers analyzed, three were identified as the most stable, as illustrated in Fig. 2. In the A-Conformer, the adsorbent is positioned near ST's chlorine atoms. For the B-Conformer, the nanostructure is oriented parallel to the aromatic rings of ST. Lastly, in the C-Conformer,  $B_{12}N_{12}$  is located close to the amine functional group of the adsorbate. After optimizing the geometry for all configurations, it was observed that the nanocluster shifted closer to the ST structure, indicating a favorable interaction between ST and  $B_{12}N_{12}$ . Importantly, no structural

distortions occurred during this process, suggesting that the adsorption is relatively strong and can be classified as physisorption [44]. To gain deeper insights into the adsorption behavior, adsorption energy calculations were performed, with results presented in Table 1. The negative values of adsorption energy across all conformers confirm that ST's interaction with the BN nanocage is experimentally feasible. A detailed analysis of Table 1 highlights that the A-Conformer is energetically more favorable compared to B and C, as indicated by its more negative total electronic and adsorption energy values [45]. The study also examined the role of water as a solvent on adsorption energies,

Table 1. The structural properties of ST, B<sub>12</sub>N<sub>12</sub> and their complexes in gaseous and aqueous phases at room temperature

Structures	Total electronic energy (a.u)	Adsorption energy (kJ/mol)	$\nu_{\min}$ (cm <sup>-1</sup> )	$\nu_{\max}$ (cm <sup>-1</sup> )	Dipole moment (Deby)
ST (Vacuum)	-1633.216	---	85.710	4058.180	3.841
ST (Water)	-1633.225	---	81.000	4063.080	3.960
B <sub>12</sub> N <sub>12</sub> (Vacuum)	-956.165	---	537.350	1795.870	0.000
B <sub>12</sub> N <sub>12</sub> (Water)	-956.169	---	531.090	1792.220	0.030
A-Conformer (Vacuum)	-2589.399	-47.259	15.710	3990.450	5.102
A-Conformer (Water)	-2589.403	-23.630	17.930	4112.370	5.893
B-Conformer (Vacuum)	-2589.393	-31.506	23.170	4057.490	6.101
B-Conformer (Water)	-2589.400	-15.753	28.320	4077.910	6.780
C-Conformer (Vacuum)	-2589.388	-18.379	31.280	4080.430	4.567
C-Conformer (Water)	-2589.397	-7.877	30.300	4080.470	4.732

Table 2. The calculated thermodynamic parameters in both gaseous and aqueous phases in temperature range of 298-318 K at 10° intervals

Structures	$\Delta H_{ad}$ (kJ/mol)	$\Delta G_{ad}$ (kJ/mol)	$\Delta S_{ad}$ (J/mol)	$K_{th}$
A-Conformer-Vacuum-298	-42.194	-38.479	-67.620	$5.516 \times 10^{+06}$
A-Conformer-Vacuum-308	-40.394	-36.174	-70.180	$1.355 \times 10^{+06}$
A-Conformer-Vacuum-318	-38.594	-33.869	-72.740	$3.638 \times 10^{+05}$
A-Conformer-Water-298	-26.310	-12.594	-49.611	$1.609 \times 10^{+02}$
A-Conformer-Water-308	-24.510	-10.289	-51.821	$5.548 \times 10^{+01}$
A-Conformer-Water-318	-22.710	-7.984	-53.801	$2.046 \times 10^{+01}$
B-Conformer-Vacuum-298	-38.240	-44.169	-50.389	$5.477 \times 10^{+07}$
B-Conformer-Vacuum-308	-36.440	-41.864	-52.840	$1.249 \times 10^{+07}$
B-Conformer-Vacuum-318	-34.640	-39.559	-54.058	$3.127 \times 10^{+06}$
B-Conformer-Water-298	-4.606	-10.535	-62.562	$7.011 \times 10^{+01}$
B-Conformer-Water-308	-2.806	-8.230	-64.411	$2.484 \times 10^{+01}$
B-Conformer-Water-318	-1.006	-5.925	-64.984	$9.393 \times 10^{+00}$
C-Conformer-Vacuum-298	-38.240	-44.169	-50.389	$5.477 \times 10^{+07}$
C-Conformer-Vacuum-308	-36.440	-41.864	-52.840	$1.249 \times 10^{+07}$
C-Conformer-Vacuum-318	-34.640	-39.559	-54.058	$3.127 \times 10^{+06}$
C-Conformer-Water-298	-4.606	-10.535	-62.562	$7.011 \times 10^{+01}$
C-Conformer-Water-308	-2.806	-8.230	-64.411	$2.484 \times 10^{+01}$
C-Conformer-Water-318	-1.006	-5.925	-64.984	$9.393 \times 10^{+00}$

showing that while these energies become less negative in aqueous conditions, they remain negative overall. This suggests that ST adsorption is feasible in water, and the presence of water does not significantly alter the interactions [46]. The low adsorption energy values further confirm that the interaction between ST and B<sub>12</sub>N<sub>12</sub> occurs through physisorption. Furthermore, the calculated IR frequencies listed in Table 1 exhibit no negative values, affirming that all examined structures represent true local minima. Another parameter assessed was the dipole moment, which, as displayed in Table 1, increases considerably after ST interacts with the BN nanocage. This indicates that

the ST-B<sub>12</sub>N<sub>12</sub> complexes exhibit higher chemical reactivity compared to the unmodified drug without the nanostructure [47].

#### Thermodynamic properties

Thermodynamic parameters, including  $\Delta H_{ad}$ ,  $\Delta G_{ad}$ ,  $\Delta S_{ad}$ , and  $K_{th}$ , were calculated to analyze the adsorption behavior of all conformers in both gaseous and aqueous environments at three temperatures. The summarized results are presented in Table 2. Negative  $\Delta H_{ad}$  and  $\Delta G_{ad}$  values demonstrate that ST adsorption on the BN nanocage is exothermic and occurs spontaneously in both phases. Conversely, the negative  $\Delta S_{ad}$

values suggest that the process is not entropy-driven, indicating aggregation within the ST- $B_{12}N_{12}$  complexes post-interaction [40]. Furthermore, thermodynamic equilibrium constant calculations revealed that the adsorption is entirely reversible and classified as physisorption. Temperature effects on these parameters were also assessed, showing that increasing the temperature from 298 K to 318 K leads to slight increases in  $\Delta H_{ad}$  and  $\Delta G_{ad}$ , a more negative  $\Delta S_{ad}$ , and a significant decrease in  $K_{th}$ . These findings indicate that adsorption is more thermodynamically favorable at lower temperatures [41].

#### FMO Analysis

The DOS spectra of  $B_{12}N_{12}$  and its complexes with ST are depicted in Fig. 3. The pristine BN nanocage exhibits a bandgap of 6.664 eV. However, when ST is adsorbed onto its surface, the bandgap

undergoes a significant reduction, decreasing to 5.261 eV, 5.218 eV, and 4.963 eV for conformers A, B, and C, respectively. These changes correspond to percentage reductions in the bandgap ( $\% \Delta E_g$ ) of -21.049%, -21.697%, and -25.530%. Despite the notable bandgap values, this substantial decrease in the bandgap of  $B_{12}N_{12}$  upon interaction with ST indicates a remarkable improvement in its electrical conductivity, as conductivity is inversely related to the bandgap. This suggests that the BN nanocage could serve as an effective sensing material for electrochemical detection of ST [42].

The chemical hardness of ST, initially recorded at 2.657 eV, experiences a reduction to 2.631 eV, 2.609 eV, and 2.481 eV for the A, B, and C conformers, respectively, upon interacting with the BN nanocage. This decrease signifies an enhancement in chemical reactivity during the adsorption process. The negative chemical

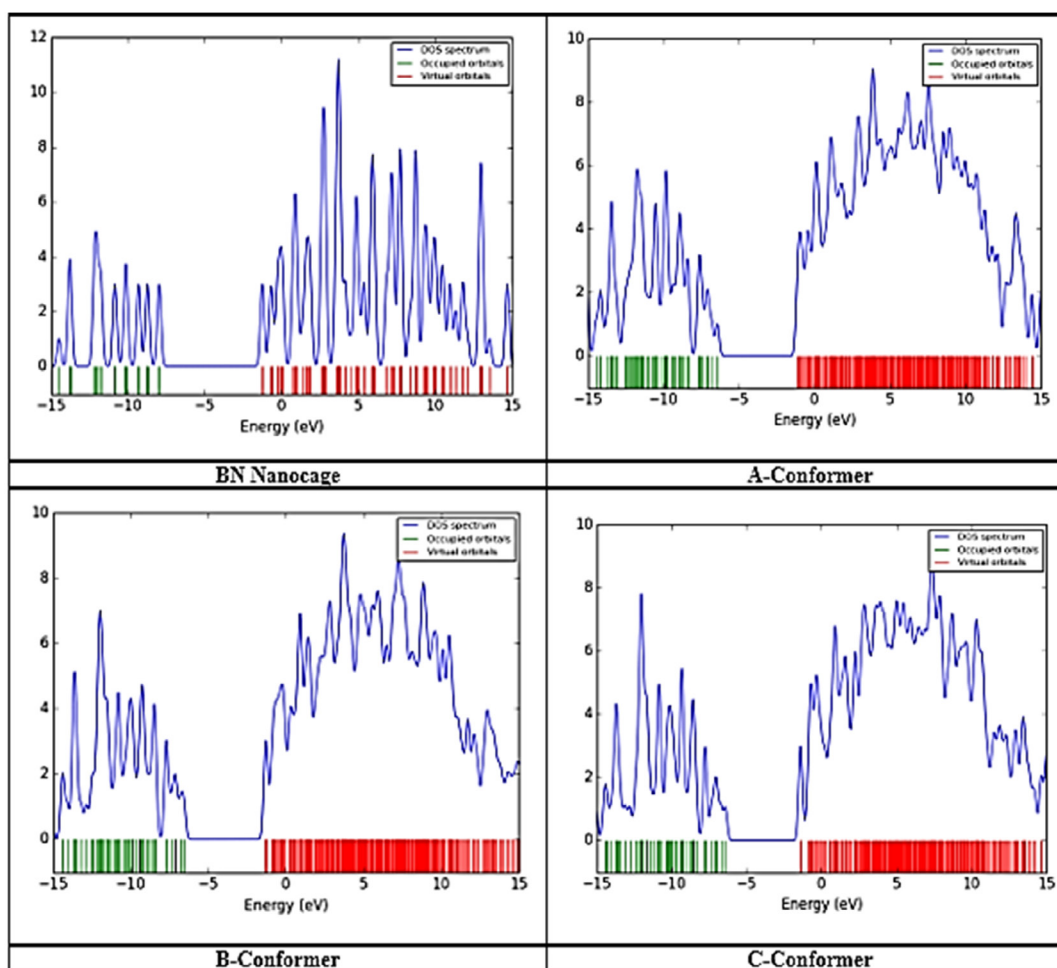


Fig. 3. The DOS spectra of  $B_{12}N_{12}$  and its complexes with ST

Table 3. The calculated FMO parameters

Structures	$E_{\text{HOMO}}$ (eV)	$E_{\text{LUMO}}$ (eV)	$E_{\text{g}}$ (eV)	% $\Delta E_{\text{g}}$	$\eta$ (eV)	$\mu$ (eV)	$\omega$ (eV)	$\Delta N_{\text{max}}$ (eV)
ST	-6.271	-0.957	5.314	---	2.657	-3.614	2.458	1.360
$B_{12}N_{12}$	-7.893	-1.229	6.664	---	3.332	-4.561	3.122	1.369
A-Conformer	-6.37	-1.109	5.261	-21.053	2.631	-3.740	2.658	1.422
B-Conformer	-6.532	-1.314	5.218	-21.699	2.609	-3.923	2.949	1.504
C-Conformer	-6.362	-1.399	4.963	-25.525	2.482	-3.881	3.034	1.564

potential values indicate that these structures are thermodynamically stable and well-suited for such interactions. Moreover, the electrophilicity indices and maximum charge transfer capacity of ST show a notable increase after adsorption on the  $B_{12}N_{12}$  surface, suggesting a stronger ability of the molecule to accept electrons [43]. This reveals that the ST- $B_{12}N_{12}$  complexes demonstrate heightened electrophilic properties compared to the original ST molecule, emphasizing their potential usefulness in applications that demand improved electron absorption capabilities [44].

## CONCLUSION

This study explores the remarkable potential of the boron nitride nanocluster, specifically  $B_{12}N_{12}$ , as an effective adsorbent and sensor for addressing the removal and detection of sertraline (ST), a widely prescribed antidepressant. Using advanced density functional theory (DFT) calculations, researchers thoroughly examined how sertraline interacts with the  $B_{12}N_{12}$  nanocluster in various orientations. The results demonstrated a strong affinity of  $B_{12}N_{12}$  for the chlorine atoms in sertraline, showcasing its selective adsorption properties. The calculated adsorption energy values, along with negative Gibbs free energy and enthalpy changes, confirmed that the interaction is not only experimentally achievable but also thermodynamically favorable. This process is exothermic and occurs spontaneously under standard conditions. Additional investigations considered external factors such as temperature and water as a solvent. Findings revealed that lower temperatures improve the adsorption process, while the interaction remains stable and efficient even in aqueous environments, highlighting its practical potential for real-world applications. Furthermore, the study examined the electronic properties of  $B_{12}N_{12}$ , revealing notable changes upon sertraline adsorption. The pristine nanocluster initially had a bandgap of 6.664 eV, which decreased significantly

to 4.963 eV after adsorption—a reduction of 25.530%. This decrease in bandgap enhances the material's electrical conductivity, making it even more suitable as a sensor. Overall, these findings suggest that  $B_{12}N_{12}$  is an excellent candidate for dual applications: acting as an adsorbent to remove sertraline from contaminated environments and serving as a sensitive sensor to detect its presence. The study provides valuable insights into the capabilities of  $B_{12}N_{12}$  nanoclusters in addressing pharmaceutical contamination and detection challenges, paving the way for future innovations in nanotechnology-based environmental and diagnostic solutions.

## CONFLICT OF INTEREST

The authors declare that there are no conflicts of interest related to the research, authorship, or publication of this manuscript. All authors have disclosed any financial or personal relationships that could potentially influence or bias the work presented.

## REFERENCES

1. Silva AL, de Sousa Sousa N, de Jesus Gomes Varela Júnior J. Theoretical studies with  $B_{12}N_{12}$  as a toxic gas sensor: a review. *J Nanopart Res.* 2023;25(1):22. <https://doi.org/10.1007/s11051-023-05667-9>
2. Pereira Silva AL, Varela Júnior JD. Density functional theory study of Cumodified  $B_{12}N_{12}$  nanocage as a chemical sensor for carbon monoxide gas. *Inorg Chem.* 2022;62(5):192634. <https://doi.org/10.1021/acs.inorgchem.2c01621>
3. Hossain MR, Hasan MM, Shamim SU, Ferdous T, Hossain MA, Ahmed F. Firstprinciples study of the adsorption of chlormethine anticancer drug on C24,  $B_{12}N_{12}$  and  $B_{12}C_6N_6$  nanocages. *Comput Theor Chem.* 2021; 1197:113156. <https://doi.org/10.1016/j.comptc.2021.113156>
4. Wu S, Li L, Liang Q, Gao H, Tang T, Tang Y. A DFT study of sulfuraphane adsorption on the group III nitrides ( $B_{12}N_{12}$ ,  $Al_{12}N_{12}$  and  $Ga_{12}N_{12}$ ) nanocages. *J Biomol Struct Dyn.* 2024;42(23):1273041. <https://doi.org/10.1080/07391102.2023.2272755>
5. Beltran LB, Ribeiro AC, Vidovix TB, Wernke G, Cusioli LF, de Mello JC, de Abreu Filho BA, Bergamasco R, Vieira AM. Zeolite functionalized with metal ions: a dual strategy for

- water purification – removal of sertraline hydrochloride and pathogenic bacteria. *Environ Nanotechnol Monit Manage.* 2025;23:101060. <https://doi.org/10.1016/j.enmm.2025.101060>
6. Koltsakidou A, Maroulas KN, Evgenidou E, Bikiaris DN, Kyzas GZ, Lambropoulou DA. Removal of the antidepressants bupropion and sertraline from aqueous solutions by using graphene oxide: a complete adsorption/desorption evaluation for singlecomponent and binary mixtures. *J Mol Liq.* 2025;:127147. <https://doi.org/10.1016/j.molliq.2025.127147>
  7. Vidovix TB, Januário EF, Bergamasco R, Vieira AM. Efficient removal of sertraline hydrochloride from wastewater using banana peels functionalized: performance adsorption, mechanisms and applicability. *Environ Technol.* 2024;45(11):211931. <https://doi.org/10.1080/09593330.2024.2164745>
  8. A) Mirderikvand N., Mahboubi-Rabbani M. Adsorptive Removal of Neomycin by Schiff Base Network1 (SNW1) Covalent Organic Framework. *J. Chem. Tech.* 2025; 1(2): 47-51. <https://doi.org/10.22034/jchemtech.2025.538158.1013> B) Kondori P., Hedayatizadeh-Omran A., Bayanati M. Adsorptive Removal of Phenazopyridine by Single-walled BN Nanotube: Batch Experimental Studies. *Medicinal and Medical Chemistry*, 2025; 2(4): 194-198. <https://doi.org/10.22034/medmedchem.2025.548229.1053> C) Al-Shemary R. S., Mahdi I. J., Hussein N. N., Hadi A. G., Baqir S. J. Sustainable Dye Removal Using Synthesized Chitosan For Reactive Black 5 Adsorption. *Chemical Research and Technology*, 2025; 2(1): 38-44. <https://doi.org/10.22034/chemrestec.2025.523466.1050> D) Mirderikvand N., Mahboubi-Rabbani M. Furazolidone Removal by Alumina Nanoparticles: Batch Experimental Studies. *Journal of Medicinal and Medical Chemistry*, 2025; 1(3): 86-90. <https://doi.org/10.22034/jmedchem.2025.544736.1017>
  9. A) Mohamadpour F, Mohamadpour F. Photodegradation of six selected antipsychiatric drugs; carbamazepine, sertraline, amisulpride, amitriptyline, diazepam, and alprazolam in environment: efficiency, pathway, and mechanism-a review. *Sustain Environ Res.* 2024;34(1):8. B) Gholami Dastnaei P. Adsorptive Removal of Neomycin by Fe<sub>3</sub>O<sub>4</sub> Nanoparticles. *Journal of Medicinal and Medical Chemistry*, 2025; 1(1): 1-6. <https://doi.org/10.22034/jmedchem.2025.221480> C) Gornik T, Kovacic A, Heath E, Hollender J, Kosjek T. Biotransformation study of antidepressant sertraline and its removal during biological wastewater treatment. *Water Res.* 2020; 181:115864. D) Sharif S. A., S. El-Mugrbi W., El-Moghrabi H. A., Mostafa M. A., Alsharkasi A., Abubakr K. A., Al Hussein R. B. A. Phytoadsorption of Lead Ions from Water Using Fava Beans Pods as Potential Bioadsorbents. *Chemical Research and Technology*, 2025; 2(2): 51-55. <https://doi.org/10.22034/chemrestec.2025.517715.1047> E) Mehraban M. Tigecycline removal by BN nanotube by batch adsorption experiments. *Journal of Medicinal and Medical Chemistry*, 2025; 1(4): 137-142. <https://doi.org/10.22034/jmedchem.2025.558910.1024>
  10. Jiao X, Lin J, Zhang R, Deng T, Yu C, Chen M, Tang C, Huang Y. Constructing of porous boron nitride granules for dynamic adsorption of CO<sub>2</sub>. *Sep Purif Technol.* 2025;131727. <https://doi.org/10.1016/j.seppur.2025.131727>
  11. Arabi S. Adsorptive Removal of Trimethoprim by Single Walled Boron Nitride Nanotube. *Journal of Medicinal and Medical Chemistry*, 2025; 1(2): 38-42. <https://doi.org/10.22034/jmedchem.2025.542592.1015>
  12. Sikri N, Behera B, Kumar A, Kumar V, Pandey OP, Mehta J, Kumar S. Recent advancements on 2D nanomaterials as emerging paradigm for the adsorptive removal of microcontaminants. *Adv Colloid Interface Sci.* 2025;103441. <https://doi.org/10.1016/j.cis.2025.103441>
  13. Vaziri I, Amini I, Poor Heravi MR, Rzaevyev R. A density functional theory study of adsorption dimethyl fumarate on the surface of the pristine gC<sub>3</sub>N<sub>4</sub> and Fe, Ni and Cu decorated graphitic carbon nitride. *Chem Rev Lett.* 2025;8(1):5267. <https://doi.org/10.22034/crl.2024.454286.1327>
  14. de Sousa Sousa N, Silva AL, Silva AC, de Jesus Gomes Varela Júnior J. Cumodified B12N12 nanocage as a chemical sensor for nitrogen monoxide gas: a density functional theory study. *J Nanopart Res.* 2023;25(12):248. <https://doi.org/10.1007/s11051-023-05898-w>
  15. Saadh MJ, Hsu C, Kareem RA, Jafarova AM, Zareii A, Edalat M, Mirzaei M. Computational assessments of 5Fluorocytosine (Flucytosine) antifungal adsorption onto a fullerene oxide nanocage for engineering a potential drug delivery platform. *Chemical Review and Letters*, 2025;8:54754.
  16. Benjamin I, Louis H, Okon GA, Qader SW, Afahanam LE, Fidelis CF, Eno EA, Ejiofor EE, Manicum AL. Transition metaldecorated B12N12-X (X= Au, Cu, Ni, Os, Pt, and Zn) nanoclusters as biosensors for carboplatin. *ACS Omega.* 2023;8(11):1000621. <https://doi.org/10.1021/acsomega.2c07250>
  17. Behjatmanesh-Ardakani R, Magkoev TT. SO<sub>2</sub> adsorption and its direct proportional dissociation on the Cu(100), Cu(110), and Cu(111) surfaces: a periodic DFT study. *Chemical Review and Letters*, 2024;7:873-83. <https://doi.org/10.22034/crl.2024.467740.1380>
  18. Gürer ES, Kaya S, Katin KP. Computational evaluation of Ni@B12N12 and Ti@B12N12 endohedral clusters as carriers for melphalan and sulforaphane anticancer drugs. *J Mol Liq.* 2025; 427:127457. <https://doi.org/10.1016/j.molliq.2025.127457>
  19. Saadh MJ, Hsu C, Kareem RA, Jafarova AM, Zareii A, Edalat M, Mirzaei M. Computational assessments of 5Fluorocytosine (Flucytosine) antifungal adsorption onto a fullerene oxide nanocage for engineering a potential drug delivery platform. *Chem Rev Lett.* 2025;8(3):54754. <https://doi.org/10.22034/crl.2025.512441.1561>
  20. Najafi F, Sattari Alamdar S, Vaziri E. Fullerene (C<sub>20</sub>) as a Sensor for the Detection of Nordazepam: DFT Simulations. *Journal of Medicinal and Medical Chemistry*, 2025; 1(1): 18-23. <https://doi.org/10.22034/jmedchem.2025.526412.1004>
  21. Behjatmanesh-Ardakani R, Rzaevyev R. Hydrogen assisted SO<sub>2</sub> dissociation on the Pt-doped graphene quantum dot surface: a non-periodic DFT study. *Chemical Review and Letters*, 2025;8:178-86. <https://doi.org/10.22034/crl.2024.489135.1476>
  22. Mirderikvand N, Mahboubi-Rabbani M. A DFT Study on Citalopram Adsorption on the Surface of B12N12. *Journal of Chemical Technology*, 2025; 1(3): 90-95. <https://doi.org/10.22034/jchemtech.2025.538393.1015>
  23. Mahdi MS, Mushtaq H, Hasan DF, Bahir H, Idan A, Hassan, Behmagham F. Electronic and optical properties of 2D VFeSb: case study by DFT. *Chemical Review and Letters*, 2024;7:964-71. <https://doi.org/10.22034/crl.2024.455831.1333>

24. Abrahi Vahed S, B12N12 as a Sensor for the Detection of Nordazepam. *Medicinal and Medical Chemistry*, 2024; 1(1): 14-19. <https://doi.org/10.22034/medmedchem.2024.474845.1008>
25. Behnia A, Jalali Sarvestani MR, Abdulmutaleb Ibrahim A, Mahdi MS. DFT studies on the nalidixic acid interactions with C8B6N6 nanocluster, *Chemical Review and Letters*, 2024;7:993-1000. doi: <https://doi.org/10.22034/crl.2024.478064.1418>
26. Ekoru I A, Osharode M E. Computational Insights into Aporphine Alkaloids as Inhibitors of Lassa fever Virus: A Molecular Modelling and DFT Approach. *Medicinal and Medical Chemistry*, 2025; (): e229565. <https://doi.org/10.22034/medmedchem.2025.544010.1049>
27. Behjatmanesh-Ardakani R, Rzaev R. Pd- and Pt-doped graphene quantum dots for SO<sub>2</sub> adsorption and dissociation: a non-periodic DFT study, *Chemical Review and Letters*, 2024;7:1022-30. <https://doi.org/10.22034/crl.2024.474971.1412>
28. Iorhuna F, Ayuba AM, Nyijime AT. Comparative study of skimmianine as an adsorptive inhibitor on Al (110) and Fe (111) crystal surface using DFT and simulation method, *Journal of Chemistry Letters*, 2023;4:148-55. <https://doi.org/10.22034/jchemlett.2023.398506.1117>
29. Dennington R, Keith TA, Millam JM. GaussView, Version 6.1. Semichem Inc., Shawnee Mission, KS. 2016.
30. Frisch MJ, Trucks GW, Schlegel HB, Scuseria GE, Robb MA, Cheeseman JR, et al. Gaussian 16, Revision C.01. Gaussian, Inc., Wallingford CT. 2016.
31. Orto M, Pantazis DA, Neese F. Density functional theory. *Photosynthesis Research*. 2009; 102:443-453. <https://doi.org/10.1007/s11120-009-9404-8>
32. Rassolov VA, Pople JA, Ratner MA, Windus TL. 6-31G\* basis set for atoms K through Zn. *The Journal of Chemical Physics*. 1998;109(4):1223-1229. <https://doi.org/10.1063/1.476673>
33. Hoseyni SJ, Karbakhshzadeh A, Moshtaghi Zonouz A, Hussein B. Computational investigation on interaction between graphene nanostructure BC3 and antiparkinson drug amantadine: possible sensing study of BC3 and its doped derivatives on amantadine, *Chemical Review and Letters*, 2024;7:380-87. <https://doi.org/10.22034/crl.2024.454413.1328>
34. Abrahi Vahed S. Fullerene (C20) as a Sensor for Detection of Midazolam: Theoretical Insights. *Journal of Medicinal and Medical Chemistry*, 2025; 1(3): 106-110. <https://doi.org/10.22034/jmedchem.2025.547513.1019>
35. Alimohammadi F, Rezanejaded Bardajee G, Monfared A. The sensing behavior of MgO nanotube to thiopropamine drug via DFT investigation, *Chemical Review and Letters*, 2024;7:513-21. <https://doi.org/10.22034/crl.2024.457011.1335>
36. Mohammadi B, Jalali Sarvestani MR. A comparative computational investigation on amantadine adsorption on the surfaces of pristine, C-, Si-, and Ga-doped aluminum nitride nanosheets, *Journal of Chemistry Letters*, 2023;4:66-70. <https://doi.org/10.22034/jchemlett.2023.388369.1107>
37. Hsian RL, Hussin V K, Hamad O A, Kareem R O. Theoretical Study Chlorohydroquinone with substituted lithium via Quantum Computation Methods, *Chemical Research and Technology*, 2024; 1(2): 73-77. <https://doi.org/10.2234/chemrestec.2024.448968.1009>
38. John A, Uzairu A, Shallangwa G, Adamu UBA, S. Theoretical investigation and design of novel cephalosporin-based inhibitors of a DD-carboxypeptidase enzyme of *Salmonella typhimurium*, *Journal of Chemistry Letters*, 2023;4:52-58. <https://doi.org/10.22034/jchemlett.2022.361586.1085>
39. Jameel RK, Al-Anbari HA, Mansoor AS, Kadhem AH, Bahair H, Behmagham F, Abbasi V. Characterization of tetramethyl guanidinium 4-nitro phenoxide (TMG-NP) and tetraphenyl guanidinium 4-nitro phenoxide (TPG-NP) as new ionic liquids (ILs) using DFT and ab initio, *Chemical Review and Letters*, 2024;7:661-76. <https://doi.org/10.22034/crl.2024.465452.1368>
40. Uzah T, Timothy M, Mbonu IJ. Insight into synergistic corrosion inhibition of thiourea and ZnCl<sub>2</sub> on mild steel: experimental and theoretical approaches, *Journal of Chemistry Letters*, 2024;4:211-21. <https://doi.org/10.22034/jchemlett.2024.413932.1135>
41. Ahmadi R. Furazolidone Adsorption on the Surface of B12N12: DFT Simulations. *Journal of Medicinal and Medical Chemistry*, 2025; 1(3): 100-105. <https://doi.org/10.22034/jmedchem.2025.547065.1018>
42. Kareem RO, Hamad OA, Kebiroglu H, Mohammed BA. Spectroscopic properties and computational studies of phosphosilicate-doped compounds including (F, Cl, Br), *Journal of Chemistry Letters*, 2024;5:159-67. <https://doi.org/10.22034/jchemlett.2024.467720.1212>
43. Issofa P, Eric N Njankwa, Gabriel C S K, Junior Ulrich B B J, Emadak A. Theoretical Mechanistic and Kinetic Study on the [1. 5]-H Shift in (Z)-hexa-1,3-diene. *Chemical Research and Technology*, 2024; 1(2): 89-94. <https://doi.org/10.22034/chemrestec.2024.449583.1012>
44. Rafiee MA, Javaheri M. Theoretical study of benzoquinone derivatives as organic cathode materials in lithium-ion batteries, *Journal of Chemistry Letters*, 2025;6:166-74. <https://doi.org/10.22034/jchemlett.2025.516569.1295>
45. Shamsadini F. S., Halvani P., Nouraddini L., Hoseininezhad-Namin M. S. Non-linear optical and theoretical properties of some isatin thioketal derivatives. *Medicinal and Medical Chemistry*, 2024; 1(2): 64-70. <https://doi.org/10.22034/medmedchem.2024.477667.1011>
46. Mirderikvand N., Bayanati M. Chlorpromazine Adsorption on the Surface of Fullerene (C20): DFT Insights. *J. Chem. Tech*, 2025; 1(4): 167-172. <https://doi.org/10.22034/jchemtech.2025.552799.1027>
47. Noqani H., Behnia A. Clomipramine Interaction with B12N12: DFT Simulations. *Journal of Medicinal and Medical Chemistry*, 2025; 1(4): 118-123. <https://doi.org/10.22034/jmedchem.2025.558192.1022>